

Polarimetry of ϵ Aurigae, From November 2009 to January 2012

Gary M. Cole

*Starphysics Observatory, 14280 W. Windriver Lane, Reno, NV 89511;
garycole@mac.com; www.starphysics.com*

Received March 20, 2012; revised May 17, 2012; accepted June 25, 2012

Abstract During the 2010–2012 eclipse of ϵ Aurigae, the author obtained linear polarization measurements during 200 nights of observation over three observing seasons. These observations began before second contact and have extended some six months into the post-eclipse period. Measurements were made in V, B, and R photometric bands. The polarization of ϵ Aurigae was observed to vary by nearly 0.6% peak to valley during this period in cycles of varying duration. These variations resemble, at a qualitative level, those seen by Kemp and Henson during the 1984 eclipse egress. In particular they show evidence of local polarization activity extending well past 4th contact.

1. Introduction

ϵ Aurigae is an F-type supergiant star approximately 2,000 light years distant. Normally seen at magnitude 3, it undergoes an 18-month-long eclipse every 27 years. The secondary object acts as an opaque disk, partially covering the primary, which dims the system's light by approximately one magnitude. While the disk is assumed to contain a hot embedded star, the spectrum of the secondary has not been observed.

At the suggestion of Dr. Robert Stencel (University of Denver) in May 2009, the author began a series of broadband polarimetric observations of ϵ Aur during its recent eclipse. The purpose was to extend measurements obtained during the 1984 eclipse by Dr. Jim Kemp and colleagues (Kemp *et al.* 1986) and followed up by his student, Dr. Gary Henson (Henson 1989).

Those observations had revealed significant variations in polarization during and after the eclipse. Dr. Stencel suggested that similar observations during the recent eclipse should be useful for comparison.

Observations reported herein were made over the course of three observing seasons. Season 1 from November 2009 to February 2010, season 2 from September 2010 to May 2011, and season 3 from July 2011 into January 2012. Ongoing instrument development led to significant improvements in the quality of measurements over the course of this work.

2. Instrumentation

There are no commercial sources for small telescope astronomical polarimeters. My instruments have been purpose-built for this project following the general concepts used on the Hawaii 88-inch telescope as described in Masiero *et al.* (2007).

An imaging telescope becomes a dual beam polarimeter with the introduction of a rotating half wave retarder and a calcite beamsplitter. The waveplate material used is an achromatic polymer of the same specification as in the Hawaii instrument. The beamsplitter is a 13-mm calcite Savart plate fabricated by Halbo Optics, which provides a separation of 1 mm at the CCD focal plate. This is approximately 135 arcseconds at the plate scale used on the C8 telescope and 55 arcseconds on the C14. This is more than enough to cleanly separate the slightly defocused and astigmatic star images. The initial waveplate rotator was constructed with a USB-controlled servo motor and plastic gearing.

The Savart plate and a focal reducer were mounted into the nose of an SBIG ST6 camera. The rotator, BVR filter selector, and camera were attached to a C8 optical tube and the entire assembly was mounted onto an existing automated C14 telescope.

This arrangement was used for the first season of observing. For the second season, the camera was replaced with a SBIG ST402 camera. This greatly reduced thermal noise and reduced download time. The rotator, which had frequent breakdowns and poor gearing, remained in use until February of 2010 when it was replaced with a high precision rotator engineered by Optec, Inc.

For the final season of this work, the instrument was reconfigured to work in the C14 optical system. The waveplate rotator was mounted between the focuser and the existing four-way instrument selector. A double fold orthogonal mirror assembly relays the beam into the Savart + camera assembly.

These ongoing changes have yielded significant improvements in data quality over the course of this project. In the first season of measurements, the uncertainty, Δp , in the degree of linear polarization was $\sim \Delta p \pm 0.1\%$; in the second season this was improved to $\sim \Delta p \pm 0.05\%$, and further refined to $\sim \Delta p \pm 0.03\%$ in the third.

Note: The Johnson BVR photometric filters are used in series with a 400-700nm luminance filter so as to match the effective range of the achromatic waveplate. This results in a slightly reddened B and a slightly truncated R bandpass.

3. Calibration

A Polarimeter can exhibit systematic error due to 1) instrumental polarization, 2) co-ordinate frame miss-alignment, and 3) modulation inefficiency.

Instrumental polarization is detected by observing zero polarization standard stars. Several hundred measurements of such stars indicate that such instrumental effects, if present, are less than 0.03% and show no preferred orientation.

The angle of polarization, θ , is defined by IAU conventions as an angle from the North-South line, towards East. The measured angle, therefore, must be adjusted so as to maintain this convention. The first level of adjustment is to set the “zero point” of the waveplate to replicate the convention. This was done using an externally-mounted sheet polarizer oriented along the declination axis. A second step was to refine the fiduciary angle by using measurements of standard stars.

In practice, the author has found it very difficult to maintain the angular precision of the instrument over the course of these observations. Frequent rotator breakdowns, mechanical rotation, and reconfigurations have disturbed the effective alignment and hence the reported angles. Frequent observations of HD 21291, whose stability was affirmed from HPOL measurements (U. Wisconsin 2012), were used for angular correction.

The modulation efficiency was checked by comparing large sets of instrumental results with catalog values for stars of known high polarization. The results obtained match expected values within the experimental uncertainties. No corrections for modulation efficiency have been made.

4. Observing procedure

An automated procedure has been developed for collecting and reducing the data for each measurement and posting the results to a summary file for that object. A detailed calculation report and all data files are retained.

The telescope is slewed to the target. A filter is selected and an initial image frame is taken. The image is dark-subtracted and the target star pair is located.

An appropriate exposure time is calculated based upon the maximum pixel level of the original image. Three dark images are obtained from which a median dark image is assembled. The system then collects from four to eight data sets, each consisting of four data frames taken at different waveplate positions. Each frame is dark-subtracted using the median dark for the series.

The entire sequence is repeated using a shorter exposure time if any pixel in any image exceeds a preset sub-saturation threshold.

The original rotator was stepped through angular positions of 0, 22.5, 45, and 67.5 degrees for each set because moving in a consistent direction minimized gear errors. Once the new rotator was installed the images were taken in 0, 45, 22.5, 67.5 order so that the pairs of images used to determine each of the two Stokes parameters were taken as closely in time as possible. The waveplate was then stepped by 90 degrees for each subsequent data set to minimize the effects of any irregularities in the angular setting of the waveplate.

5. Data reduction

A floating square aperture that is aligned to the centroid of each star is sized to capture 97.5% of the total signal on the first frame. This aperture size is then used for all images in the data set. A larger concentric aperture is used to estimate the background signal. The dual beam method is self-calibrating and does not require flat fielding, but this is subject to the requirement that the star images are recorded onto the same pixel locations within each data pair. To maintain this requirement, any data sets that have excessive motion between frames are excluded from calculations.

Once the intensity values have been extracted from all data sets of the observation, the degree of polarization and angle are computed according to the methods of Tinbergen (1996). The same are calculated for each individual data set for comparison. The error that can be ascribed to photon statistics is calculated according to the method of Serkowski (1974).

The polarization value is adjusted for zero point bias according to the method described by Clarke (2010). The value of this adjustment is typically less than 0.01% for our observations and insignificant in terms of the uncertainty associated with each measurement; the S/N ratio is high and the value of p is large relative to the measurement uncertainties.

6. Target observations

In Table 1 the result for 200 nights of observation are presented. Each measurement consists of multiple sets of four images taken at waveplate positions of 0, 22.5, 45, and 67.5 degrees. On many nights in which several measurements were obtained, these have been averaged. The errors estimated for each polarization measurement are stated in the adjoining columns. The angles are shown in the rightmost three columns. The errors associated with the angles are discussed in the next section.

7. Sources of uncertainty

Observations prior to March of 2011 were subject to imprecise waveplate positioning. The original rotating device used plastic gears to translate servo motion. As each cog of the main gear corresponds to nearly 3 degrees, a small range of random variation is inevitable. There was also an infrequent problem of “hopping.” According to the analysis done by Ramaprakash *et al.* (1998), any uncertainty of angular positioning generates a polarization uncertainty of similar magnitude. Hence if a ± 1 degree error actually occurred from time to time, it would add 0.05% to the uncertainty of an individual measurement. This source of this problem was reduced by at least a factor of 25 when the Optec Rotator was installed late in season 2.

Observations from this site encounter significant turbulence, bad seeing, wind buffeting, and imperfect guiding. The effects of seeing are to move the center of illumination and to change the distribution of light within each star image. These factors induce small random errors into the results that are difficult to quantify. An examination of the reported variations in closely-spaced time sequential measurements suggest that the data carry error about 50% greater than predicted simply from the photon flux.

For the data presented in this paper, the errors reported in the table and charts for each measurement are double those calculated based upon the photon statistics of the actual images. The author believes this provides a conservative estimate of the true uncertainty in total polarization.

The uncertainty in reported angles of polarization is much worse than that of the magnitude of polarization because 1) it is derived from measurements of standard stars which have at least equivalent uncertainty, and 2) because there were frequent mechanical adjustments made during the course of observations. The author believes that the angles reported contain both random and systematic errors that may reach the level of ± 1 degree.

8. Discussion

The polarization measurements (%) in the *BVR* photometric bands are plotted as a time series in Figure 1. The first season of observations covers the time approaching the second contact during the eclipse. The polarization values (p) are high and are matched again in the early part of the second half of the second season leading up to the end of the eclipse. The third observing season is beyond the eclipse phase and shows strong polarization activity with falls and recoveries covering several tens of days with amplitudes much the same as during the eclipse. Particularly on the protracted fall of some 70 days at the beginning of the second season, soon after mid-eclipse, the color dependence of the polarization clearly shows in Figure 1, with the values of p falling from *B* through *V* to *R*.

Figure 2 displays p and the position angle, θ , for the *V* band over the three seasons. There appears to be a correlation between the three peaks of p and troughs in θ during the second season, but this is not quite as apparent post-eclipse. This behavior indicates that the variable intrinsic polarization is at a significant angle to that of the large interstellar component.

Several researchers, including the team at the Pine Bluff Observatory of the University of Wisconsin, have made synoptic, out-of-eclipse observations of this binary system. During 1990 to 1996, their measurements revealed $p(V)$ values varying from 1.96% to 2.06% with $\theta(V) \sim 144$ degrees. This we assume to be the interstellar component.

Figure 3 displays the normalized Stokes parameters q and u as a function of time. Direct comparison of the polarimetric behavior of this eclipse with

that reported by Kemp *et al.* (1986) of the previous one cannot be made as the earlier authors provide normalized Stokes parameter time-line plots with the q, u values expressed in a co-ordinate frame at 5 degrees relative to the standard equatorial system. However, as the angular difference between frames is very small, strong qualitative comparisons can be made.

In particular, the behavior of both q and u during the egress phase is extremely similar with small oscillations in q and a smooth rise in u in both data sets followed by a rapid decline. The magnitude and frequency of variation in both data sets show considerable similarity but not direct repetition except at egress.

A standard method for investigation of polarimetric data is to plot the normalized Stokes parameters q, u as Cartesian co-ordinates. This has been done in Figure 4 for all the V-band data. Although the scatter of the plotted points is very large, simple inspection shows that there is a trend. This becomes more readily apparent when the data are grouped into smaller temporal segments as has been done in Figure 5. While each segment has a different origin in the q, u -plane, the slopes during these four selected time intervals are close to being parallel. This is shown more clearly in Figure 6 where the four segments are overlaid. Translating these gradients into celestial angles, the polarizational movement appears along position angles between 7 and 22 degrees. Given the level of error in the raw data, these values are close to that (5 degrees) taken by Kemp *et al.* (1986) from the astrometric data of van de Kamp (1978) as being related to the orbital plane direction projected on to the sky. The uncertainty of this angle is not given by Kemp *et al.* (1986) and it is difficult to ascertain the best value from the sketch provided by van de Kamp (1978). As the trend angles are close to the estimate of the orbital projection angle, short-term polarization changes, chiefly affecting the q values, can be surmised as originating from scattering by clumpy material in the orbital plane. The drifts may be affected by introduction of new clumps and their decay, or by changes in their distance from the illuminating star. As to why the origin of the trend lines moves about to produce the more blurred picture that Figure 5 presents, with significant changes in the u parameter, a more sophisticated model is required.

Finally, there appears to be correlation however between several of the U band photometric maxima of the recent eclipse (ϵ Aur campaign 2011) and the polarimetric maxima in these data. In particular, at JD 2455460, at JD 2455545, and at egress the values of U and p seem to move together.

9. Future work

In future seasons it is the author's intention to monitor the system in the same frequent manner as during the eclipse to confirm the nature of the variability and search for short-term periodicities. A simultaneous program of U and B photometry will be added to search for any direct correlation between the optical and polarimetric variability.

10. Acknowledgements

The author extends his thanks to Dr. Robert Stencel of the University of Denver, without whose thoughtful advice and encouragement this project would not have been completed. Also thanks to Dr. Stencel for kindly providing a copy of Henson (1989).

Thanks also to Bolder Vision Optik, of Boulder, Colorado, for the waveplate materials and to Optec, Inc., Lowell, Michigan, for the design and fabrication of the waveplate rotator.

This research has made use of the SIMBAD and VizieR databases operated at CDS, Strasbourg, France and of NASA's Astrophysics Data System.

The author acknowledges the Citizen Sky project of the AAVSO and the National Science Foundation.

References

Clarke, D. 2010, *Stellar Polarimetry*, Wiley-VCH, Hoboken, NJ.
 ϵ Aurigae campaign. 2011, <http://www.hposoft.com/Plots09/UBBand.jpg>.
 Henson, G. D. 1989, Ph.D. dissertation (September), Univ. Oregon.
 Kemp, J. C., Henson, G. D., Kraus, D., Beardsley, I., Carroll, L., Ake, T., Simon, T., and Collins, G. 1986, *Astrophys. J., Lett. Ed.*, **300**, L11.
 Masiero, J., Hodapp, K., Harrington, D., and Lin, H. 2007, *Publ. Astron. Soc. Pacific*, **119**, 1126.
 Ramaprakash, A. N., Gupta, R., Sen, A. K., and Tandon, S. N. 1998, *Astron. Astrophys., Suppl. Ser.*, **128**, 369.
 Serkowski, K. 1974, in *Planets, Stars, and Nebulae Studied With Photopolarimetry*, ed. T. Gehrels, Proc. IAU Collq. 23, Univ. Arizona Press, 136.
 Tinbergen, J. 1996, *Astronomical Polarimetry*, Cambridge Univ. Press, Cambridge, 100.
 Univ. Wisconsin, Space Astronomy Laboratory. 2012, HPOL spectropolarimeter website (<http://www.sal.wisc.edu/HPOL/>).
 Van de Kamp, P. 1978, *Astron. J.*, **83**, 975.

Table 1. Observations of ϵ Aurigae polarization from JD 2455145 to 2455944 in V, B, and R photometric bands.

<i>JD</i>	<i>V %Pol</i>	<i>%Err</i>	<i>B %Pol</i>	<i>%Err</i>	<i>R %Pol</i>	<i>%Err</i>	<i>V θ</i>	<i>B θ</i>	<i>R θ</i>
2455145	2.474	0.07	—	—	—	—	—	—	—
2455150	2.482	0.05	—	—	2.381	0.1	—	—	—
2455151	2.307	0.09	—	—	—	—	—	—	—
2455154	2.259	0.11	—	—	2.22	0.04	—	—	—
2455155	2.454	0.14	—	—	2.396	0.05	—	—	—

Table continued on following pages

Table 1. Observations of ϵ Aurigae polarization from JD 2455145 to 2455944 in V, B, and R photometric bands, cont.

<i>JD</i>	<i>V %Pol</i>	<i>%Err</i>	<i>B %Pol</i>	<i>%Err</i>	<i>R %Pol</i>	<i>%Err</i>	<i>V θ</i>	<i>B θ</i>	<i>R θ</i>
2455159	2.357	0.09	—	—	2.334	0.1	—	—	—
2455168	2.145	0.05	—	—	2.147	0.09	—	—	—
2455169	2.249	0.04	—	—	2.206	0.07	—	—	—
2455191	2.218	0.1	—	—	—	—	—	—	—
2455201	2.201	0.14	—	—	—	—	—	—	—
2455202	2.112	0.08	—	—	2.208	0.09	—	—	—
2455210	2.287	0.08	—	—	2.271	0.07	—	—	—
2455211	2.314	0.1	—	—	2.246	0.14	—	—	—
2455212	2.325	0.09	—	—	—	—	—	—	—
2455220	2.271	0.04	2.299	0.06	—	—	—	—	—
2455449	2.168	0.06	2.232	0.06	2.104	0.06	139.8	138.7	140.9
2455450	2.197	0.06	2.192	0.06	2.136	0.06	140.2	139.1	141.2
2455451	2.194	0.07	2.209	0.07	2.239	0.07	139.6	140.1	139.3
2455452	2.212	0.07	2.236	0.06	2.18	0.07	139.1	138.3	140.9
2455453	2.233	0.05	2.223	0.05	2.166	0.06	139	138.3	140.8
2455454	2.238	0.07	2.233	0.06	2.148	0.07	139.5	138.4	141.1
2455455	2.176	0.04	2.215	0.03	2.132	0.04	139.3	138.7	141.3
2455456	2.208	0.04	2.225	0.04	2.193	0.04	138.9	138.9	139.5
2455458	2.222	0.05	2.293	0.05	2.183	0.05	139.2	138.2	141.3
2455462	2.244	0.06	2.27	0.06	2.138	0.06	139.2	138.3	140.6
2455463	2.193	0.05	2.264	0.04	2.136	0.05	139.1	137.7	140.7
2455464	2.246	0.06	2.262	0.05	2.309	0.06	139	138.8	139.1
2455465	2.142	0.06	2.197	0.06	2.189	0.06	138.8	138.2	138.4
2455467	2.218	0.05	2.283	0.05	2.203	0.05	139.4	138.4	140.8
2455468	2.222	0.06	2.243	0.05	2.144	0.08	139.9	139	141.3
2455469	2.188	0.06	2.198	0.06	2.179	0.06	138.9	137.6	140.7
2455470	2.144	0.07	2.191	0.06	2.085	0.07	139.6	138.9	141.2
2455478	2.154	0.05	2.171	0.05	2.117	0.06	141	139.9	143
2455479	2.12	0.06	2.193	0.05	2.127	0.06	141.2	140.3	142.3
2455480	2.118	0.07	2.105	0.07	2.119	0.06	140.5	140.7	140.7
2455481	2.125	0.06	2.135	0.06	2.07	0.06	141.2	139.9	142.7
2455482	2.13	0.07	2.149	0.07	2.117	0.07	141.8	140.5	143.1
2455483	2.142	0.06	2.142	0.06	2.097	0.07	141.8	140.8	143.5
2455484	2.133	0.06	—	—	2.168	0.07	142	—	142.9
2455485	2.148	0.06	2.154	0.06	2.119	0.06	140.9	140.3	142.8
2455489	2.114	0.06	2.101	0.06	2.068	0.07	142	140.8	142.5
2455490	2.103	0.05	2.126	0.06	2.184	0.05	140.6	140.8	140.1
2455501	2.152	0.04	2.1	0.03	2.085	0.03	141.16	140.56	142.36
2455502	2.083	0.04	2.113	0.04	2.015	0.04	141.8	141.4	143.1

Table continued on following pages

Table 1. Observations of ϵ Aurigae polarization from JD 2455145 to 2455944 in V, B, and R photometric bands, cont.

<i>JD</i>	<i>V</i> %Pol	%Err	<i>B</i> %Pol	%Err	<i>R</i> %Pol	%Err	<i>V</i> θ	<i>B</i> θ	<i>R</i> θ
2455503	2.093	0.05	2.127	0.04	2.05	0.06	142	141.2	143.8
2455504	2.082	0.05	2.057	0.05	2.044	0.07	141.4	141	142.7
2455505	2.083	0.06	—	—	—	—	141.8	—	—
2455507	2.063	0.04	2.065	0.03	2.029	0.04	140.8	140.1	142.9
2455509	2.083	0.05	2.081	0.07	2.076	0.06	142.2	141.8	145
2455512	2.042	0.06	2.029	0.05	1.993	0.05	142.6	142	144.7
2455513	2.036	0.06	2.031	0.06	1.962	0.06	141.9	140.7	143.6
2455514	2.063	0.07	—	—	2.041	0.09	141.2	—	142.9
2455515	2.111	0.08	2.043	0.07	2.004	0.07	141.2	141.6	143.4
2455516	2.1	0.06	2.025	0.05	2.022	0.06	141.2	140.4	142.5
2455517	2.061	0.06	2.045	0.06	2.026	0.06	141	141	142.3
2455518	2.031	0.06	—	—	—	—	141.8	—	—
2455532	2.225	0.06	2.189	0.04	2.186	0.05	140	139.9	141.9
2455537	2.234	0.06	2.266	0.06	2.214	0.06	138.1	137.5	138.7
2455542	2.278	0.07	2.328	0.06	2.158	0.07	145.1	146	146.5
2455543	2.262	0.05	2.285	0.04	2.205	0.04	137.1	136.4	138.4
2455547	—	—	—	—	2.175	0.06	—	—	138.8
2455554	2.246	0.08	2.219	0.05	2.146	0.07	137.4	136.1	140
2455555	2.246	0.06	2.243	0.06	2.174	0.06	137.3	136.3	139.3
2455558	2.154	0.07	2.199	0.06	2.207	0.08	138	136.9	140.7
2455565	2.115	0.05	2.15	0.05	2.091	0.05	139.7	139.5	141.6
2455566	2.122	0.05	2.124	0.05	2.021	0.05	138.7	137.8	140.7
2455567	2.122	0.06	2.104	0.05	2.064	0.06	138.4	137.6	140.2
2455568	2.113	0.05	2.102	0.04	2.015	0.05	139	138.2	140.9
2455569	2.149	0.05	2.112	0.06	2.088	0.05	138.3	138.5	139
2455570	2.16	0.04	2.113	0.04	2.101	0.04	140.2	139.4	142.8
2455576	2.198	0.07	2.223	0.06	2.194	0.07	139.6	139.1	141.3
2455577	2.316	0.06	2.342	0.04	2.297	0.06	140.1	140.7	141.7
2455578	2.355	0.06	2.239	0.05	2.262	0.06	141.3	140.2	141.2
2455579	2.278	0.06	2.221	0.06	2.197	0.06	140.8	140.2	142.3
2455581	2.304	0.07	2.257	0.06	2.281	0.06	141.2	140.7	142.3
2455582	2.316	0.06	2.297	0.05	2.243	0.06	141	140.6	141.5
2455583	2.336	0.06	2.289	0.05	2.307	0.06	140.7	140.9	142.7
2455584	2.293	0.06	2.274	0.06	2.246	0.05	140.5	140.1	142.9
2455587	2.355	0.07	2.269	0.06	—	—	140.6	140.2	—
2455588	2.297	0.06	2.24	0.05	2.232	0.06	139.9	140.1	141.3
2455589	2.281	0.05	2.277	0.06	2.228	0.06	140.2	139.9	142.5
2455593	2.312	0.06	2.332	0.06	2.27	0.06	139.7	139.3	142.1
2455595	2.257	0.07	2.192	0.06	2.394	0.06	138.4	138.2	140.6

Table continued on following pages

Table 1. Observations of ϵ Aurigae polarization from JD 2455145 to 2455944 in V, B, and R photometric bands, cont.

JD	V %Pol	%Err	B %Pol	%Err	R %Pol	%Err	V θ	B θ	R θ
2455596	2.359	0.07	2.367	0.07	2.229	0.07	137.8	138.8	139.6
2455597	2.362	0.06	2.343	0.05	2.3	0.05	138.4	138.1	139.3
2455599	2.372	0.06	2.385	0.05	2.253	0.06	137.5	137.5	139.6
2455600	2.425	0.05	2.385	0.04	—	—	137.7	137	—
2455602	2.405	0.08	2.463	0.06	2.34	0.06	136.3	134.9	137.7
2455615	2.298	0.08	2.338	0.07	2.278	0.06	136.65	137.35	136.45
2455616	2.312	0.05	2.289	0.03	2.264	0.04	137.15	137.45	137.05
2455620	2.177	0.05	2.192	0.04	2.159	0.04	138.75	138.85	138.55
2455621	2.184	0.07	2.193	0.04	2.221	0.05	138.85	139.15	138.25
2455629	2.008	0.06	1.995	0.05	1.961	0.08	140.65	141.15	139.35
2455630	1.971	0.04	1.971	0.04	1.949	0.05	140.31	141.41	139.81
2455632	2.03	0.06	—	—	—	—	139.21	—	—
2455633	1.946	0.04	1.922	0.03	1.914	0.04	141.03	141.23	140.73
2455638	1.913	0.07	—	—	1.873	0.06	145.13	—	145.13
2455643	1.872	0.07	1.9	0.06	—	—	—	—	—
2455649	1.975	0.08	1.971	0.05	2.002	0.06	141.24	141.14	140.54
2455651	2.019	0.05	1.988	0.05	2.012	0.05	143.04	142.94	142.24
2455652	2.025	0.04	1.983	0.05	2.013	0.05	141.93	142.03	140.83
2455653	1.979	0.07	2.011	0.06	1.991	0.08	139.63	141.73	140.03
2455654	1.99	0.04	1.959	0.04	1.979	0.04	141.93	141.93	140.83
2455655	1.978	0.07	2.003	0.09	2.005	0.08	141.73	143.03	141.13
2455656	2.005	0.07	1.977	0.06	1.953	0.08	142.83	143.53	141.53
2455657	1.994	0.08	2.01	0.07	2.006	0.07	144.13	144.93	144.23
2455659	2.031	0.05	2.014	0.03	2.028	0.05	142.43	141.73	141.93
2455661	1.96	0.07	—	—	—	—	147.93	—	—
2455662	2.011	0.07	1.996	0.08	2.037	0.06	141.98	142.38	140.38
2455663	2.017	0.05	2.03	0.05	2.02	0.05	142.38	141.88	140.68
2455665	2.021	0.03	2.008	0.04	—	—	142.38	141.68	—
2455667	1.997	0.05	2.017	0.08	—	—	141.38	142.08	—
2455670	1.959	0.08	1.924	0.06	—	—	141.58	140.98	—
2455673	1.937	0.08	—	—	—	—	140.68	—	—
2455676	2.024	0.05	2.048	0.06	—	—	139.68	140.38	—
2455678	2.025	0.05	1.925	0.07	—	—	140.98	140.88	—
2455679	2.058	0.07	2.004	0.07	1.988	0.06	140.98	140.58	140.18
2455682	2.034	0.06	2.004	0.06	2.004	0.06	141.58	141.68	141.98
2455683	2.036	0.09	2.035	0.1	2	0.11	140.58	144.28	139.68
2455684	2.005	0.09	2.069	0.07	—	—	142.38	141.08	—
2455685	1.99	0.06	2.034	0.06	2.025	0.07	142.08	141.58	141.48
2455686	2.017	0.07	—	—	—	—	141.18	—	—

Table continued on following pages

Table 1. Observations of ϵ Aurigae polarization from JD 2455145 to 2455944 in V, B, and R photometric bands, cont.

<i>JD</i>	<i>V</i> %Pol	%Err	<i>B</i> %Pol	%Err	<i>R</i> %Pol	%Err	<i>V</i> θ	<i>B</i> θ	<i>R</i> θ
2455687	2.118	0.06	—	—	—	—	141.28	—	—
2455762	—	—	2.111	0.04	2.026	0.04	—	144.5	146.6
2455765	2.108	0.03	2.133	0.03	—	—	145.5	145.2	—
2455766	2.094	0.03	—	—	2.077	0.03	145.5	—	144
2455767	2.172	0.03	—	—	—	—	143.3	—	—
2455768	2.125	0.02	—	—	—	—	142.8	—	—
2455769	2.187	0.03	2.181	0.03	2.091	0.03	143.7	144	145.6
2455770	2.161	0.03	2.162	0.02	2.099	0.02	143.4	143.2	144.8
2455771	2.175	0.03	2.148	0.03	2.143	0.03	143.9	144	144.8
2455775	2.203	0.03	2.178	0.03	2.106	0.03	143.8	143.6	145
2455776	2.183	0.03	—	—	2.086	0.02	142.7	—	143.4
2455777	2.137	0.02	2.151	0.02	2.148	0.02	142.5	142.3	142.7
2455778	2.114	0.03	2.132	0.02	2.107	0.02	142.4	143	142.6
2455779	2.118	0.03	2.086	0.02	2.052	0.02	142.9	142.4	144.5
2455780	2.085	0.02	2.086	0.02	2.026	0.02	142.7	142.1	143.7
2455781	2.068	0.03	2.087	0.03	2.051	0.02	143	142.8	144.4
2455782	2.069	0.03	2.072	0.02	1.997	0.03	142.4	141.3	143.6
2455783	2.062	0.03	2.015	0.03	2.056	0.03	141.3	141	141.3
2455784	2.047	0.03	2.077	0.03	2.025	0.02	141.5	141.5	141.2
2455785	2.058	0.03	2.053	0.03	2.018	0.02	142.6	141.8	140.7
2455788	2.054	0.02	2.015	0.02	1.988	0.02	141.8	141.1	142.8
2455789	2.026	0.03	2.003	0.02	1.968	0.02	143.1	142.8	142.7
2455790	2.012	0.03	2.011	0.02	1.986	0.03	142.1	141.2	143.1
2455791	2.063	0.03	2.012	0.02	1.998	0.02	141.6	140.6	142.6
2455792	2.047	0.03	1.992	0.02	1.988	0.03	141.3	140.9	141.7
2455793	2.047	0.02	2.025	0.03	2.006	0.02	141.2	140.6	142.3
2455794	2.05	0.03	1.948	0.03	2.012	0.03	141	140	142.2
2455795	2.057	0.03	2.054	0.03	1.948	0.04	140.8	139.8	141.8
2455796	2.033	0.03	1.973	0.03	1.984	0.03	141.3	141.3	142.4
2455798	2.015	0.03	1.962	0.03	1.935	0.03	141.4	140.4	141.8
2455799	2.003	0.04	1.94	0.03	1.935	0.03	142.6	141.9	143.4
2455801	1.999	0.03	1.939	0.03	1.453	0.03	141.7	141.2	—
2455802	1.999	0.02	1.943	0.02	1.951	0.02	142	141.7	—
2455803	1.976	0.03	1.96	0.02	1.944	0.02	143.1	142.9	143.8
2455821	—	—	1.902	0.03	—	—	—	143.9	—
2455822	1.974	0.03	1.862	0.03	1.91	0.03	143.8	144.2	145.3
2455823	1.947	0.03	1.891	0.03	1.924	0.03	145.4	145.5	145.5
2455824	1.946	0.03	1.878	0.03	1.91	0.03	145.3	145	146
2455825	1.927	0.03	1.874	0.03	1.895	0.03	145.5	145.3	146.2

Table continued on next page

Table 1. Observations of ϵ Aurigae polarization from JD 2455145 to 2455944 in V, B, and R photometric bands, cont.

JD	V %Pol	%Err	B %Pol	%Err	R %Pol	%Err	V θ	B θ	R θ
2455851	2.07	0.04	2.011	0.03	2.049	0.03	—	—	—
2455853	2.043	0.04	2.019	0.03	2.001	0.03	—	—	—
2455854	2.037	0.03	2.056	0.03	2.025	0.03	145.56	144.36	143.66
2455856	2.036	0.04	2.03	0.04	2.037	0.03	142.41	143.21	142.81
2455857	2.02	0.03	2.063	0.03	1.943	0.03	142.72	142.22	152.92
2455858	2.034	0.02	2.056	0.02	2.041	0.02	143.02	142.72	142.42
2455860	2.071	0.04	2.14	0.03	2.073	0.03	141.99	142.09	141.89
2455861	2.157	0.04	2.189	0.04	2.064	0.04	142.05	143.25	142.25
2455862	2.062	0.03	2.068	0.03	2.019	0.03	142.64	142.64	142.44
2455863	2.065	0.03	—	—	—	—	144.32	—	—
2455865	2.008	0.03	1.964	0.02	1.977	0.03	143.31	142.81	142.61
2455866	1.992	0.02	2.018	0.02	2.02	0.02	143.21	143.01	143.01
2455867	2.01	0.03	1.975	0.02	—	—	142.1	141.9	—
2455876	2.057	0.03	2.091	0.03	2.061	0.02	—	—	—
2455878	2.058	0.04	—	—	—	—	—	—	—
2455881	2.029	0.04	1.983	0.03	2.011	0.03	142.8	141.8	144.2
2455882	2.032	0.03	1.988	0.02	2.032	0.02	143.2	142.3	144.5
2455894	2.005	0.03	2.022	0.02	1.999	0.02	138.1	138.3	138.7
2455895	2.057	0.03	2.005	0.02	2.03	0.03	143.5	143.2	144.8
2455897	2.082	0.03	2.067	0.02	1.989	0.02	143.5	142.6	145.6
2455898	2.128	0.03	2.069	0.02	2	0.03	143.7	143.1	145.6
2455899	2.067	0.03	2.078	0.03	2.039	0.03	143.3	142.7	145.3
2455902	2.091	0.03	2.044	0.02	2.049	0.03	143.2	142.6	144.6
2455903	2.073	0.04	2.064	0.03	2.037	0.03	148.2	142.7	144.9
2455904	2.067	0.03	2.057	0.02	2.018	0.03	144.1	142.7	144.7
2455905	2.078	0.03	2.066	0.02	2.065	0.02	142.8	143.3	145.6
2455906	2.123	0.03	2.06	0.03	—	—	143.7	143	—
2455907	2.105	0.03	2.07	0.04	2.048	0.03	143.6	142.3	144.8
2455908	2.098	0.03	—	—	2.08	0.04	144.4	—	146.8
2455909	2.106	0.03	2.104	0.03	2.048	0.03	143.5	143.7	146.1
2455913	2.101	0.03	2.048	0.02	2.03	0.02	144.3	144	145.7
2455917	2.082	0.02	2.068	0.02	2.068	0.02	144.4	144.1	146
2455918	2.08	0.03	2.089	0.02	2.044	0.02	142.8	142.3	144.1
2455936	2.004	0.03	1.944	0.02	1.919	0.02	145.1	144.6	146.8
2455938	2.04	0.06	2	0.03	—	—	143.7	143.4	—
2455939	1.972	0.02	2.014	0.02	—	—	145.4	146.2	—
2455940	1.951	0.05	1.969	0.03	—	—	—	—	—
2455941	2.011	0.02	—	—	—	—	145.1	—	—
2455944	2.028	0.03	—	—	—	—	—	—	—

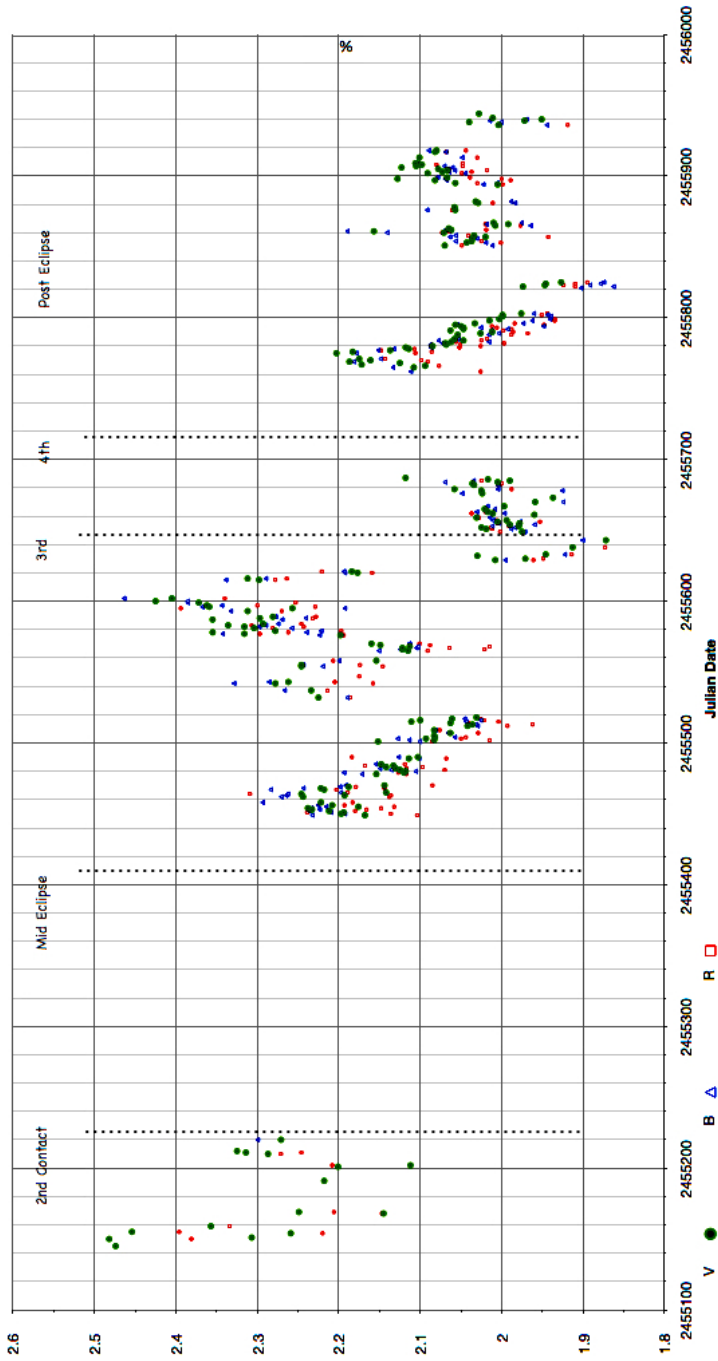


Figure 1. ϵ Aur eclipse: BVR percentage of polarization. V are circles, B are triangles, R are squares.

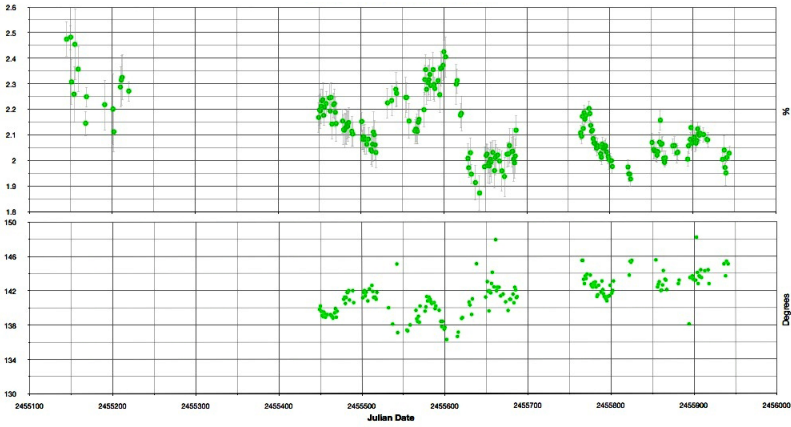


Figure 2. ϵ Aur eclipse: V percentage of polarization (p) and V position angle (θ).

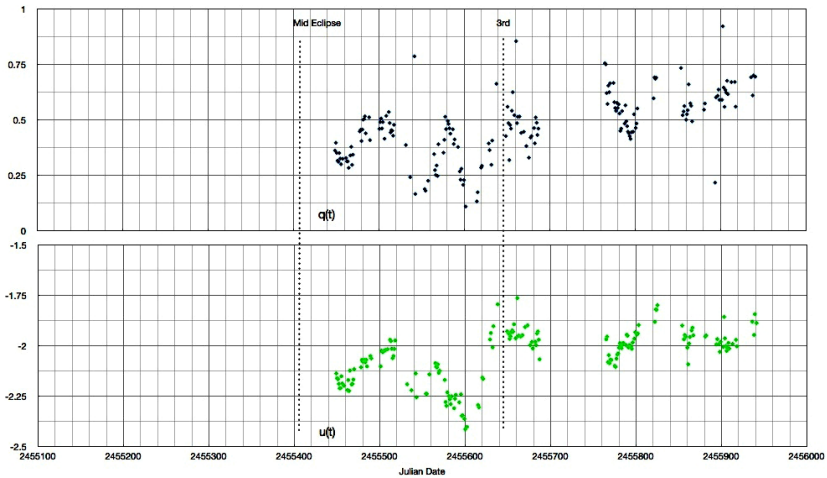


Figure 3. ϵ Aur eclipse: normalized Stokes parameters as a function of time.

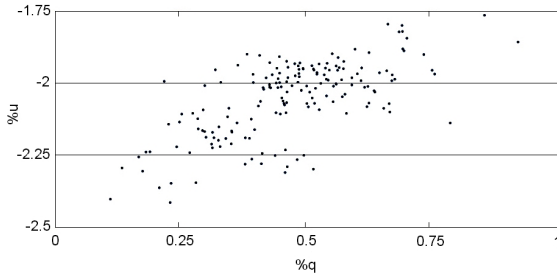


Figure 4. ϵ Aur eclipse: Stokes u as a function of q for all observations.

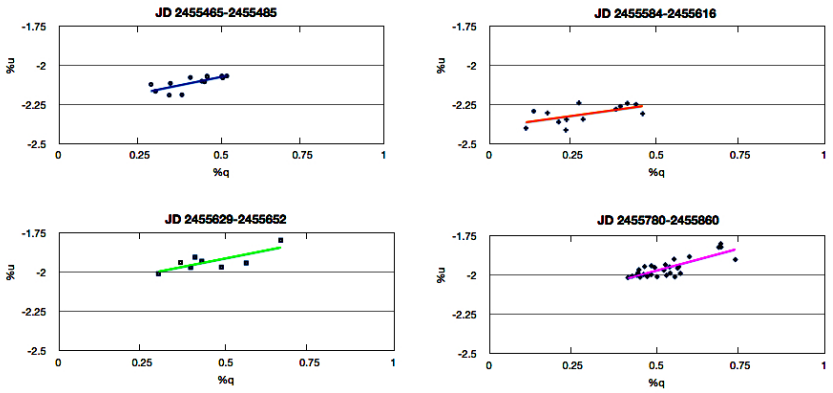


Figure 5. ϵ Aur eclipse: q,u diagrams for selected epochs.

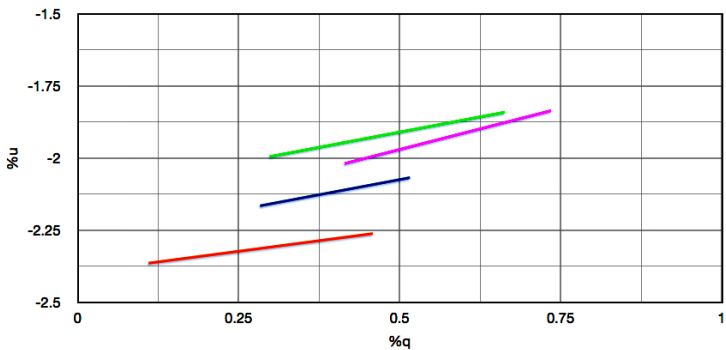


Figure 6. Overlay of q,u trendlines for selected epochs.